



Complex nearly immotile behaviour of enzymatically driven cargos†

Cite this: DOI: 10.1039/c8sm01893f

 O. Osunbayo,^{‡a} C. E. Miles,^{‡b} F. Doval,^c B. J. N. Reddy,^d J. P. Keener^{‡b} and M. D. Vershinin^{‡*c}
Received 15th September 2018,
Accepted 17th January 2019

DOI: 10.1039/c8sm01893f

rsc.li/soft-matter-journal

We report a minimal microtubule-based motile system displaying signatures of unconventional diffusion. The system consists of a single model cargo driven by an ensemble of N340K NCD motors along a single microtubule. Despite the absence of cytosolic or cytoskeleton complexity, the system shows complex behavior, characterized by sub-diffusive motion for short time lag scales and linear mean squared displacement dependence for longer time lags. The latter is also shown to have non-Gaussian character and cannot be ascribed to a canonical diffusion process. We use single particle tracking and analysis at varying temperatures and motor concentrations to identify the origin of these behaviors as enzymatic activity of mutant NCD. Our results show that signatures of non-Gaussian diffusivities can arise as a result of an active process and suggest that some immotility of cargos observed in cells may reflect the ensemble workings of mechanochemical enzymes and need not always reflect the properties of the cytoskeletal network or the cytosol.

Introduction

Microtubule-associated motility enables essential intracellular functions and processes in eukaryotic cells. Hence, observation and modeling of this process is a major modern research direction. Much less attention is devoted to studies of how cargos do not move. The temporary lack of directed cargo motion is often seen but rarely analysed in depth in particle tracking and analysis studies. It can significantly affect net cargo velocity for one particle and net cargo flux for a population of cargos. In addition, cargos driven by multiple molecular motors can remain immotile for extended periods of time at microtubule intersections due to being simultaneously bound to multiple filaments.^{1–5} In such cases, the cargos act as dynamic cross-links for the cytoskeleton and their function bridges the fields of motility and biomechanics.^{6,7} Extended stationary periods are therefore a distinct class of motile behaviour which requires extensive *in vitro*⁸ and *in silico*⁹ modeling, as well as additional experimental tools to establish the underlying root causes of such events.

Intracellular cargo tracks tend to be highly complex because motion can be driven by a variety of causes, including mechanochemical enzymes¹⁰ and passive diffusion¹¹ (equivalently, motion can be driven by causes that obey or break detailed balance¹²). The distinction between passive and active motion is crucial. For example, one might use positional fluctuations of an intracellular cargo to calibrate *in vivo* optical trapping,¹³ but it is essential to first establish that the chosen cargos are not subject to motor activity. On the other hand, if enzymatic contribution is established then one can proceed to probe the properties of molecular motors mediating the motility.^{14,15} It is thus desirable in many experimental contexts to have a simple way to distinguish between active and passive motility.

Mean-squared displacement (MSD) analysis¹⁶ is commonly used to classify single particle motion. Pure Brownian motion leads to linear MSD curves whereas motion driven by individual mechanochemical enzymes often proceeds at constant velocity and produces a quadratic MSD dependence.^{16,17} An important subtlety is that Brownian motion is not the only stochastic process that leads to linear MSD curves.^{18,19} A linear MSD can very well arise from an active process, for example, with a balanced ensemble of mechanochemical enzymes that oppose each-other's motion. Hence, MSD analysis may be convenient and easy to perform but it is not always able to distinguish active from passive motility.

Motility analysis and modeling is rapidly changing.^{19,20} Interest in active fluctuations and awareness of complications in practical data analysis is growing.^{21,22} Practical examples of enzymatically driven diffusion are now well established.¹⁵

^a Department of Biology, University of Utah, Salt Lake City, UT 84112, USA^b Department of Mathematics, University of Utah, Salt Lake City, UT 84112, USA^c Department of Physics & Astronomy, University of Utah, Salt Lake City, UT 84112, USA. E-mail: vershinin@physics.utah.edu^d Department of Developmental and Cell Biology, University of California Irvine, Irvine, CA 92617, USA

† Electronic supplementary information (ESI) available. See DOI: 10.1039/c8sm01893f

‡ OO and CM contributed equally to this work.

However, theoretical approaches to teasing out various diffusion and active motility modes from single particle tracking data¹⁸ are still under active development^{23,24} and a single standardized approach has yet to emerge. It is however clear that in general mere tracking and associated analysis is insufficient to relate cargo-scale phenotype to constituent single molecule contributions. There is thus an acute need for new experimental probes of complex motility.

In this work, we construct a minimal experimental model of an active but apparently diffusive process. We establish that the process is active by demonstrating the diffusion coefficient's dependence on motor concentration, as well as the requirement for ATP presence in the system. We then examine the resulting motility and demonstrate that even in our minimal system the overall ensemble phenotype is complex. We further show how active contribution to the apparent diffusion can be isolated *via* a simple experimental approach. Finally, we argue *via* additional experimental and theoretical analysis that this type of complex behaviour is likely more general than our minimal model system.

Materials and methods

Bead assays

Taxol stabilized microtubules were deposited on a glass coverslip, washed, then coverslip surface was blocked and the bead/motor sample was subsequently admitted into the flow cell, as previously described.²⁵ Briefly, glass coverslips were coated with poly-L-lysine, and attached to sapphire slides (Swiss Jewel Company, Philadelphia, PA) *via* double-sided tape (3 M, Maplewood, MN). Taxol stabilized microtubules (MT) were diluted into the flow buffer and then deposited into flow cell and incubated for 15 min. The flow buffer was PMEE (35 mM Pipes, 5 mM MgSO₄, 1 mM EGTA, 0.5 mM EDTA) supplemented with 20 μM taxol and 1 mM GTP. Excess MTs were then washed away and the surface was blocked with buffer containing 22 mg mL⁻¹ casein (Sigma-Aldrich, St. Louis, MO). For the temperature-dependent experiments carboxylated \varnothing 1 μm polystyrene beads (Polysciences, Warrington, PA) were incubated with excess NCD N340K kinesin diluted in PMEE buffer augmented with 105 mM of NaCl, 5 mM of ATP and 5 mM Dithiothreitol and incubated at 4 °C for 30 min. For the motor concentration-dependent experiments, the lower concentration was 0.13 μM while the higher concentration was 10× greater, 1.3 μM. In all cases, beads were observed to bind to microtubules without detachment during the entire observation period consistent with multiple NCD motors tethering the beads to microtubules. Control beads without NCD did not bind to microtubules in a parallel assay.

Imaging and temperature control

Motility data was collected in a biologically relevant temperature range as previously described.²⁶ Briefly, flow cells were constructed as usual but sapphire window was used in place of the cover glass. A customized Peltier thermoelectric stage

(PE120; Linkam, Tadworth, UK) was placed in direct contact with the sapphire cover glass for maximum heat conductivity between the assay and the stage. Dry condenser was used to minimize thermal coupling to the microscope. Imaging was performed at ~20 fps. Bead positions were then extracted and analysed *via* custom tracking software (Matlab, Mathworks, Natick, MA).

Lipid droplet imaging

Lipid droplet motion was imaged in wild type COS1 (ATCC CRL-1650) cells *via* Differential Interference Contrast microscopy. COS1 cell culture was carried out as previously described.²⁷ Briefly, cells were grown in DMEM (Invitrogen, Carlsbad, CA) supplemented with 10% fetal bovine serum and 1% antibiotic at 37 °C in 5% CO₂. For imaging purposes, cells were attached to the polylysine coated glass coverslip by placing the coverslip at the bottom of a 60 mm Petri dish just before plating the cells. The cells were attached to the coverslip at least 6 hours before imaging. A sample chamber was constructed to facilitate the imaging as previously described.²⁷ Live cell imaging was performed at 30 frames per s. Lipid droplets were tracked *via* custom software (Matlab, Mathworks, Natick, MA).

MSD analysis of bead motion

Bead displacements were video recorded at $\Delta t \sim 20$ fps. Bead location in each frame was extracted²⁸ and full bead trajectory was then reconstructed for each bead (*e.g.* Fig. 1A and B). For each trajectory, squared displacements between all location pairs whose time points were separated by a specific time interval

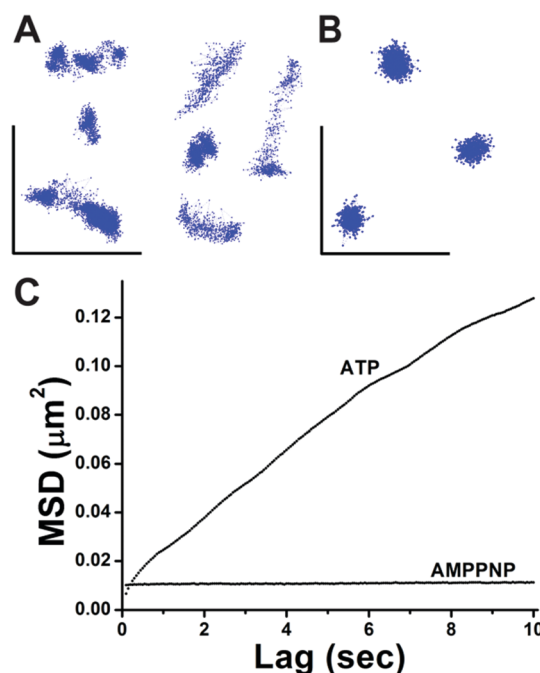


Fig. 1 Bead motility at room temperature. Representative weakly motile tracks in the ATP (A) and AMPPNP (B) background. Scale bars: 1 μm. (C) Mean-square displacement (MSD) for motion in ATP and AMPPNP background (as indicated).

(time lag) were averaged to calculate mean squared displacement for each time lag of interest.

The uncertainty in MSD values for a given time lag were estimated by pooling all such values for all independent bead trajectories (for a specific experimental condition). One sigma and two sigma confidence intervals could then be estimated from this data set non-parametrically (necessary because these distributions were clearly not Gaussian).

Linear fits were performed for lag times between 1 and 3 seconds. Longer time lags were penalized in the fit because variance between MSDs for particle trajectories grows with lag.¹⁷ Our regression also used inverse estimated variance as fitting weights¹⁷ to improve estimation. A few exceptional trajectories showed motion consistent with ballistic (constant velocity) transport. Akaike information criterion was used to filter out MSD curves which fit quadratic model better than the linear one. Inclusion of such trajectories is somewhat ambiguous in principle, since a linear fit need not produce a meaningful estimate, but in practice it does not substantially alter the results above.

Protein purification

N340K mutant of NCD with N-terminal 6xHis tag was bacterially expressed in BL21DE3. Lysis was accomplished by sonication for 45 min at 4 °C. Lysis buffer: 50 mM Tris pH 7.5, 300 mM NaCl, 10% glycerol, 20 mM imidazole, 10 μM PMSF, 2 mM βME with EDTA-free Roche mixture inhibitors. Cell lysis was followed by immobilized metal ion affinity chromatography purification (two washes and elution). Wash buffer 1: 50 mM Tris pH 7.5, 700 mM NaCl, 10% glycerol, 40 mM imidazole, 0.02% Triton X-100, 2 mM βME. Wash buffer 2: 50 mM Tris pH 7.5, 300 mM NaCl, 10% glycerol, 75 mM imidazole, 2 mM βME. Elution buffer: 25 mM Tris pH 7.5, 300 mM NaCl, 10% glycerol, 500 mM imidazole, 2 mM βME. Gene synthesis/purification were performed by Bionexus, Inc.

Results and discussion

We have examined a bead assay in which a single cargo is driven along a single filament by multiple copies of a single type of motor: N340K mutant of kinesin-14 NCD (non-claret disjunctional).²⁹ Wildtype NCD is non-processive with a bias for minus-end directed powerstroke.^{29–33} The N340K mutant is a bi-directional motor, with more balanced preference for stepping in either direction. Ensembles of N340K NCD motors were previously used in a microtubule gliding assay and showed ensemble bi-directional motility. Most of the motility was reported to be localized but some contiguous displacements in either direction were too long to be ascribed to diffusion even though overall motile random process appeared roughly stationary.²⁹ The general view regarding this phenomenon is that the cooperative activity of NCD motors is sufficient to temporarily power directed displacement¹² but the choice of direction occurs *via* spontaneous symmetry breaking and need not be biased in a specific direction. However, diffusive motion has not been fully ruled out.¹¹

We studied NCD N340K driven motility in a bead assay to more closely model active bi-directional cargo motion (Fig. 1). The observed motility was consistent with gliding assay phenotype:²⁹ most beads exhibited limited localized motions while some beads had more extensive bi-directional motility. The MSD analysis of tracks revealed that the motion is strongly sub-diffusive on short time scales but apparently diffusive on longer time scales (Fig. 1).

The characteristic diffusion coefficient we observed at room temperature is $0.008 \mu\text{m}^2 \text{s}^{-1}$ – more than an order of magnitude lower than the typical diffusion coefficients for regular diffusion of proteins along microtubules.^{11,34} However in a system with multiple cross-bridges between the cargo and the filament this is not quite definitive. We then asked whether the linear MSD lineshape could be directly attributed to the enzymatic activity of NCD. We repeated the study in the AMPPNP (rather than ATP) background. In this case the MSD curve was nearly flat, suggesting that apparent diffusion and enzymatic activity were abolished concomitantly (Fig. 1).

It is natural to attribute the enzymatic activity which underlies apparent diffusion described above to NCD N340K motors: they are the only ATPases present under our controlled conditions and the only cargo-filament crossbridges present (no cargo binding was seen in assays absent the motors). However, it was not *a priori* as clear whether this was a collective phenomenon, although prior theoretical work suggested that it was and that the variation of effective diffusivities with the number of motors should be experimentally observable.³⁵ We therefore tested motility at two motor concentrations separated by an order of magnitude. We found that the distributions of effective diffusion coefficients were significantly different, with significantly more apparently diffusive motion observed at the lower concentration (Fig. 2). This answers our question regarding the linear MSD lineshape, leading us to indeed attribute it to the ensemble activity of ATP-driven motor enzymes.

The linear fits¹⁷ to long lag time portion of the MSD curves revealed that the distribution of the effective diffusion coefficients

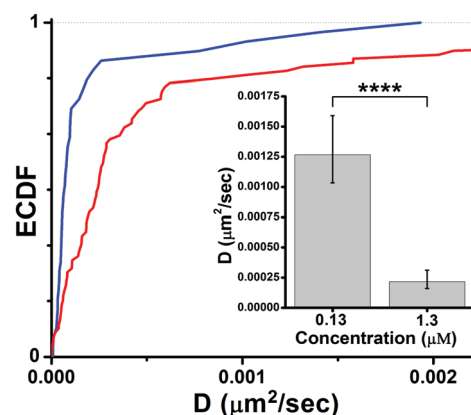


Fig. 2 Effective diffusion dependence on motor concentration. Empirical cumulative distribution function (ECDF) for motors at 0.13 μM (red) and 1.3 μM (blue) motor concentrations. (inset) Maximum likelihood estimates for characteristic diffusion coefficient assuming exponential distribution. Error bars: 95% c.i. ($p < 1 \times 10^{-4}$).

is not Gaussian. At all temperatures it is highly skewed and reasonably approximated by an exponential distribution (Fig. 2 and 3A). This feature is unexpected: approximately Gaussian distributions typically arise in this type of analysis due to the central limit theorem for large data sets. Indeed, this observation is in contrast to *e.g.* simple Brownian motion of beads in water, for which the distribution of diffusion coefficients is of course approximately Gaussian and varies slowly with temperature (Fig. S1, ESI[†]). Though exponential density is unusual, it does provide us with a decay scale which we can then use as the characteristic of diffusion at a given temperature.

Non-Gaussian distribution of diffusivities has been reported in many systems with linear average MSD character³⁶ but not for enzymatically driven ensembles. We conclude that active matter is subject to similar puzzling behaviours as passive matter. How then can we test whether the source of apparent diffusion is passive or active? We sought methodology to answer this question which could be readily used *in vivo* as well as *in vitro*. The central idea behind our approach is that biological enzymes typically undergo dramatic changes in activity over a biologically relevant temperature range^{26,36,37} whereas passive processes like ordinary diffusion show much less pronounced variation with temperature (Fig. S1, ESI[†]). We demonstrate (Fig. 3) that temperature dependent single particle tracking is indeed a rapid and convenient approach for analysing the active contribution to apparent diffusion.

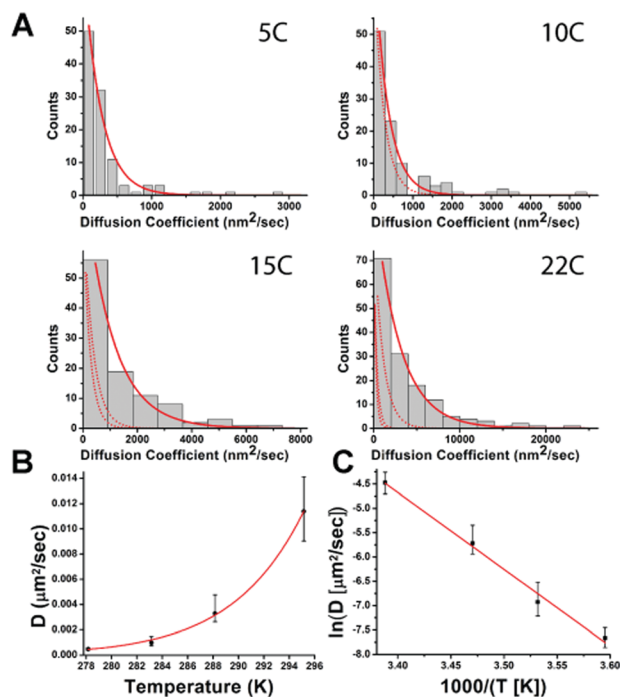


Fig. 3 Temperature dependence of apparent diffusion coefficients. (A) Histograms of diffusion coefficients for 5, 10, 15, 22 °C are shown as labelled. In each panel, a fit to exponential density is shown (solid red). Because x-axis values needed to be rescaled for data at variable temperatures, fits to exponential densities at lower temperatures are shown for higher temperature panels (dashed red) for reference of overall scale. Characteristic diffusion coefficient for each temperature and a best fit Arrhenius curve (red) are shown on linear (B) and Arrhenius style (C) plots.

The characteristic diffusion coefficients from assays in a biologically relevant temperature range yielded an excellent fit to the Arrhenius model but not to the linear one (Fig. 3B and C). The activation energy extracted from the Arrhenius fit was 130 KJ mol⁻¹ – somewhat high but within the range of activation energies observed for kinesin motors especially for a system of multiple motors where a stepping enzyme would see significant opposing load.³⁸ It is unlikely that another energy barrier relevant to our system is in this range. For example, the activation energies for protein diffusion along the microtubule lattice are not generally precisely known but are thought to be more than an order of magnitude lower.¹¹ The energy barriers relevant for the motor-microtubule detachment are of order 10 KJ mol⁻¹.³⁹ Therefore, variable temperature measurements are sufficient to detect the active process contributing to the apparent diffusion.

The last question we aimed to address is the unexpected finding that the distribution of effective diffusion coefficients in our assays is extremely skewed. To test whether this is a more general phenomenon associated with immotile but actively driven cargos we have examined a lipid droplet motility system in mammalian COS1 cells. Lipid droplet motility is known to be driven by kinesin-2 and dynein motors⁴⁰ and is also known to show a diverse array of phenotypes, from long distance directed motion to more stationary displacements (Fig. 4). Moreover, lipid droplet motility in mammalian cells has been used as a probe of viscoelasticity of the cytoskeleton.⁴¹ Indeed, sub-diffusive behaviour has been found at short time scales but transition to linear MSD curves have been seen at longer time scales.⁴¹

We examined the lipid droplet motility at long time scales only and focused on apparently diffusive transport – MSDs which conformed to a quadratic model better than linear as per Akaike information criterion were ignored in our analysis. The resulting tracks are not all stationary: linear or sub-diffusive MSD curves can arise from active motion if it is saltatory, or if it is a minor part of a longer record. All these cases are seen in Fig. 4A. The average MSD curve is broadly consistent with a linear trend (Fig. 4B). Any minor sub-diffusive curvature for short lags is not significant although such a feature would be expected from and consistent with a prior report.⁴¹ However, the distribution of apparent diffusion coefficients (Fig. 4C) is inconsistent with Brownian motion and is instead highly skewed. The strong similarity between these observations and our *in vitro* data is of course insufficient to infer the microscopic picture of lipid droplet motility in cells. It is however sufficient to call into question whether viscoelastic contributions can be unambiguously attributed to the cytoskeletal filaments or cytosol in general. They may be partially or even wholly due to the motor contribution instead. It is also sufficient to call into question whether cytoskeletal motor contribution to nanoscale biomechanics in cells is purely elastic.⁴²

The observation of complex behaviour for nearly-immotile ensembles of molecular motors likely has some system-specific origins. At the same time, we might expect some skewness for the distribution of diffusion coefficients on very general grounds.

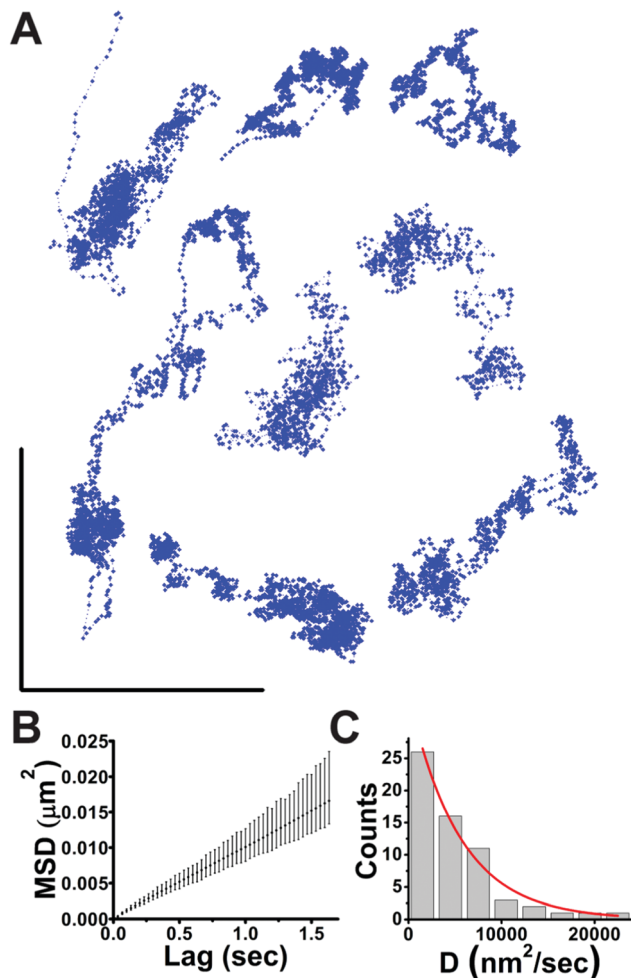


Fig. 4 Apparently diffusive subset of lipid droplet motility in COS1 cells. (A) Representative droplet tracks at 37 °C (blue). (B) The average MSD curve and (C) the distribution of effective diffusion coefficients for lipid droplets which do not show active motion. Fit to exponential density is shown in red. Scale bars in (A): 1 μm .

The active process or processes are likely to possess their own distinct length and time scales (*e.g.* for motors these scale reflect the ATPase rate and the powerstroke distance). Heterogeneity of scales and the resulting complex diffusive energy landscape can give rise to non-Gaussian diffusivities.³⁵ We consider a theoretical model with all experimental complexity reduced to just one active and one passive process⁴³ in the ESI† (Supp. Text S1 and Fig. S2, S3) and readily confirm that the skewness in this case is considerably higher than for pure diffusion.

Conclusions

We have demonstrated that cytoskeleton motor ensembles can lead to complex motile behaviours in the absence of the cytosol, in the absence of microtubule movement,⁶ and indeed even in the absence of tug of war between different motor types^{44,45} or multiple cytoskeletal filaments.⁷ Some of the motility we observed (short lag times) is clearly in the class of anomalous diffusion (Supp. Text S2 and Fig. S2, ESI†) while longer lag time motility

remains to be fully understood. We also show that active processes in the context of cytoskeletal transport can lead to linear MSD curves for longer lag times, however the apparent diffusion coefficients extracted from such MSD curves are likely to possess a highly skewed distribution. We note that inherently non-Gaussian distribution of apparent diffusion coefficients has been observed in many systems and has been recently modelled using the diffusing diffusivities approach.²⁰ This type of model is unlikely to be generally applicable for all *in vitro* and *in vivo* situations but can be extended to include active matter contribution. It is also clear that the skewness of the distribution of diffusion coefficients can clearly arise from both passive and active contributions.

Subdiffusion (without aging effects⁷) observed in the context of cytoskeletal transport has often been conceptualized as a process of cargos getting trapped in small spatial compartments and occasional jumps between such compartments.⁴⁶ Our work suggests that stationary segments of cytoskeletal cargo motion may not always be due to compartment trapping but dynamic motor-based trapping instead. In addition, models of molecular motor transport often assume motor crosslinks to be purely elastic springs.^{47,48} This assumption is convenient, computationally efficient, and allows for reasonably faithful modeling of motor-driven transport. However our observation of subdiffusive transport attributable directly to the motors (rather than the cytosolic influences) suggests that a more detailed model may be warranted.

On a practical level, we show that when dealing with cytoskeletal motility experiments which produce linear MSD curves, it is a good idea to examine the distribution of effective diffusion coefficients because deviations from Gaussian (or high-degree-of-freedom chi-squared) behaviour can be a signature of a more complex process. We show that these anomalies can arise even in minimal systems with a small ensemble of identical enzymes so that they may be pervasive in biological active matter. We further show that varying temperature is an excellent and easily experimentally accessible technique for probing active contributions to single particle motion in the cytoskeletal context.

Conflicts of interest

There are no conflicts to declare.

Acknowledgements

We would like to thank Dr S. P. Gross for insightful discussions. This work was supported by National Science Foundation grant number ENG-1563280 to M. V. BJNR was supported by grant RO1GM064624 to S. P. Gross at UC Irvine. CM and JPK were supported by NSF grants DMS 1515130 and DMS-RTG 1148230.

References

- O. Osunbayo, J. Butterfield, J. Bergman, L. Mershon, V. Rodionov and M. Vershinin, *Biophys. J.*, 2015, **108**, 1480–1483.
- J. L. Ross, H. Shuman, E. L. F. Holzbaur and Y. E. Goldman, *Biophys. J.*, 2008, **94**, 3115–3125.

- 3 A. T. Lombardo, S. R. Nelson, M. Y. Ali, G. G. Kennedy, K. M. Trybus, S. Walcott and D. M. Warshaw, *Nat. Commun.*, 2017, **8**, 15692.
- 4 M. Vershinin, B. C. Carter, D. S. Razafsky, S. J. King and S. P. Gross, *Proc. Natl. Acad. Sci. U. S. A.*, 2007, **104**, 87–92.
- 5 J. Snider, F. Lin, N. Zahedi, V. Rodionov, C. C. Yu and S. P. Gross, *Proc. Natl. Acad. Sci. U. S. A.*, 2004, **101**, 13204–13209.
- 6 I. M. Kulić, A. E. X. Brown, H. Kim, C. Kural, B. Blehm, P. R. Selvin, P. C. Nelson and V. I. Gelfand, *Proc. Natl. Acad. Sci.*, 2008, **105**, 10011–10016.
- 7 M. Scholz, S. Burov, K. L. Weirich, B. J. Scholz, S. M. A. Tabei, M. L. Gardel and A. R. Dinner, *Phys. Rev. X*, 2016, **6**, 011037.
- 8 N. D. Derr, B. S. Goodman, R. Jungmann, A. E. Leschziner, W. M. Shih and S. L. Reck-Peterson, *Science*, 2012, **338**, 662–665.
- 9 A. Kunwar, S. K. Tripathy, J. Xu, M. K. Mattson, P. Anand, R. Sigua, M. Vershinin, R. J. McKenney, C. C. Yu, A. Mogilner and S. P. Gross, *Proc. Natl. Acad. Sci. U. S. A.*, 2011, **108**, 18960–18965.
- 10 R. D. Vale, *Cell*, 2003, **112**, 467–480.
- 11 J. R. Cooper and L. Wordeman, *Curr. Opin. Cell Biol.*, 2009, **21**, 68–73.
- 12 F. Jülicher and J. Prost, *Phys. Rev. Lett.*, 1995, **75**, 2618–2621.
- 13 A. G. Hendricks, E. L. F. Holzbaur and Y. E. Goldman, *Proc. Natl. Acad. Sci.*, 2012, **109**, 18447–18452.
- 14 V. Soppina, A. K. Rai, A. J. Ramaiya, P. Barak and R. Mallik, *Proc. Natl. Acad. Sci. U. S. A.*, 2009, **106**, 19381–19386.
- 15 C. Lin, M. Schuster, S. C. Guimaraes, P. Ashwin, M. Schrader, J. Metz, C. Hacker, S. J. Gurr and G. Steinberg, *Nat. Commun.*, 2016, **7**, 11814.
- 16 H. Qian, M. P. Sheetz and E. L. Elson, *Biophys. J.*, 1991, **60**, 910–921.
- 17 M. J. Saxton, *Biophys. J.*, 1997, **72**, 1744–1753.
- 18 R. Metzler, J.-H. Jeon, A. G. Cherstvy and E. Barkai, *Phys. Chem. Chem. Phys.*, 2014, **16**, 24128–24164.
- 19 B. Wang, S. M. Anthony, S. C. Bae and S. Granick, *Proc. Natl. Acad. Sci.*, 2009, **106**, 15160–15164.
- 20 A. V. Chechkin, F. Seno, R. Metzler and I. M. Sokolov, *Phys. Rev. X*, 2017, **7**, 021002.
- 21 S. Shinkai and Y. Togashi, *EPL*, 2014, **105**, 30002.
- 22 H. Vandebroek and C. Vanderzande, *Soft Matter*, 2017, **13**, 2181–2191.
- 23 A. Robson, K. Burrage and M. C. Leake, *Philos. Trans. R. Soc. London, Ser. B*, 2013, **368**, 20120029.
- 24 M. Lysy, N. S. Pillai, D. B. Hill, M. G. Forest, J. W. R. Mellnik, P. A. Vasquez and S. A. McKinley, *J. Am. Stat. Assoc.*, 2016, **111**, 1413–1426.
- 25 T. E. Smith, W. Hong, M. M. Zachariah, M. K. Harper, T. K. Matainaho, R. M. Van Wagoner, C. M. Ireland and M. Vershinin, *Proc. Natl. Acad. Sci. U. S. A.*, 2013, **110**, 18880–18885.
- 26 W. Hong, A. Takshak, O. Osunbayo, A. Kunwar and M. Vershinin, *Biophys. J.*, 2016, **111**, 1287–1294.
- 27 B. J. N. Reddy, M. Mattson, C. L. Wynne, O. Vadpey, A. Durra, D. Chapman, R. B. Vallee and S. P. Gross, *Nat. Commun.*, 2016, **7**, 12259.
- 28 J. P. Bergman, M. J. Bovyn, F. F. Doval, A. Sharma, M. V. Gudheti, S. P. Gross, J. F. Allard and M. D. Vershinin, *Proc. Natl. Acad. Sci. U. S. A.*, 2018, **115**, 537–542.
- 29 S. A. Endow and H. Higuchi, *Nature*, 2000, **406**, 913–916.
- 30 K. A. Foster, A. T. Mackey and S. P. Gilbert, *J. Biol. Chem.*, 2001, **276**, 19259–19266.
- 31 K. Furuta and Y. Y. Toyoshima, *Curr. Biol.*, 2008, **18**, 152–157.
- 32 T. G. Wendt, N. Volkmann, G. Skiniotis, K. N. Goldie, J. Müller, E. Mandelkow and A. Hoenger, *EMBO J.*, 2002, **21**, 5969–5978.
- 33 A. E. Butterfield, R. J. Stewart, C. F. Schmidt and M. Skliar, *Biophys. J.*, 2010, **99**, 3905–3915.
- 34 M. H. Hinrichs, A. Jalal, B. Brenner, E. Mandelkow, S. Kumar and T. Scholz, *J. Biol. Chem.*, 2012, **287**, 38559–38568.
- 35 B. Wang, J. Kuo, S. C. Bae and S. Granick, When Brownian diffusion is not Gaussian, <https://www.nature.com/articles/nmat3308>, accessed September 13, 2018.
- 36 K. Kawaguchi and S. Ishiwata, *Biochem. Biophys. Res. Commun.*, 2000, **272**, 895–899.
- 37 A. L. Fink and S. J. Cartwright, *CRC Crit. Rev. Biochem.*, 1981, **11**, 145–207.
- 38 C. Bustamante, Y. R. Chemla, N. R. Forde and D. Izhaky, *Annu. Rev. Biochem.*, 2004, **73**, 705–748.
- 39 S. Uemura, K. Kawaguchi, J. Yajima, M. Edamatsu, Y. Y. Toyoshima and S. Ishiwata, *Proc. Natl. Acad. Sci.*, 2002, **99**, 5977–5981.
- 40 A. Herms, M. Bosch, B. J. N. Reddy, N. L. Schieber, A. Fajardo, C. Rupérez, A. Fernández-Vidal, C. Ferguson, C. Rentero, F. Tebar, C. Enrich, R. G. Parton, S. P. Gross and A. Pol, *Nat. Commun.*, 2015, **6**, 8176.
- 41 S. Yamada, D. Wirtz and S. C. Kuo, *Biophys. J.*, 2000, **78**, 1736–1747.
- 42 I. Goychuk, V. O. Kharchenko and R. Metzler, *Phys. Chem. Chem. Phys.*, 2014, **16**, 16524–16535.
- 43 C. E. Miles, S. D. Lawley and J. P. Keener, *SIAM J. Appl. Math.*, 2018, **78**, 2511–2532.
- 44 S. P. Gross, M. A. Welte, S. M. Block and E. F. Wieschaus, *J. Cell Biol.*, 2002, **156**, 715–724.
- 45 M. J. I. Müller, S. Klumpp and R. Lipowsky, *Proc. Natl. Acad. Sci. U. S. A.*, 2008, **105**, 4609–4614.
- 46 S. M. A. Tabei, S. Burov, H. Y. Kim, A. Kuznetsov, T. Huynh, J. Jureller, L. H. Philipson, A. R. Dinner and N. F. Scherer, *Proc. Natl. Acad. Sci.*, 2013, **110**, 4911–4916.
- 47 F. Berger, C. Keller, S. Klumpp and R. Lipowsky, *Phys. Rev. Lett.*, 2012, **108**, 208101.
- 48 A. Kunwar, M. Vershinin, J. Xu and S. P. Gross, *Curr. Biol.*, 2008, **18**, 1173–1183.